Journal of Magnetic Resonance **139,** 232–239 (1999)
Article ID jmre.1999.1802, available online at http://www.idealibrary.com on IDEAL®

High-Resolution Four-Dimensional HMQC-NOESY-HSQC Spectroscopy

Robert C. Morshauser and Erik R. P. Zuiderweg[1]

Biophysics Research Division, Department of Biological Chemistry and Department of Chemistry, University of Michigan, 930 North University Avenue, Ann Arbor, Michigan 48109

Received December 7, 1998; revised May 5, 1999

Practical optimization of the 4D [^{1}H, ^{13}C, ^{13}C, ^{1}H] HMQC-NOESY-HSQC experiment in terms of distribution of resolution over the indirect dimensions is analyzed in detail. Recommendations for an optimal experiment are based on computer simulations assessing the effective resolution of the experiment, defined as the percentage of all possible NOE cross peaks that can be assigned unambiguously on the basis of the spectral data alone. Using actual ^{13}C–^{1}H spectra of an 18-kDa chaperone protein, the analysis shows that experiments with the best effective resolution are also among the most sensitive ones. When combined with an efficient aliasing scheme that reduces indirect spectral space 124-fold, a 4D experiment that yields unambiguous assignments for 41% of all possible NOE cross peaks can be recorded in 28 h. A high-resolution experiment, which can be recorded in 8 days, yields 61% unambiguous assignments and can be analyzed more easily using standard NMR display software. The predictions are verified with experimental 4D spectra from which 1850 NOEs (914 long-range) were extracted for the 18-kDa chaperone protein.

Key Words: **four-dimensional NMR; proteins; resolution; aliasing; optimization; NOE.**

The possibility of extracting more useful information from 2D and 3D NMR spectra than from 1D NMR spectra is rarely disputed. However, this assessment is in general not extrapolated to include 4D spectra. The most common objections against 4D NMR are the lack of sensitivity, lack of resolution, length of data acquisition, and nonintuitive data handling. Most of these arguments are true, but they can also be held against 3D NMR compared to 2D NMR.

While spectra of lower dimensionality almost always have higher intrinsic sensitivity, such spectra often cannot be interpreted for larger molecules because of overlap. Thus intrinsic sensitivity does not translate to practical sensitivity. Similarly, while potentially very high resolution can be obtained in lower dimensionality spectra, resonance linewidths for larger proteins become a factor, leading to a low effective resolution due to overlap. In general, one reaches limits of effective sensitivity and resolution with 3D NOE spectra when proteins of 20 kDa and larger are studied. A case in point was the analysis in our lab of the structural NOE spectra of the substrate binding domain of a Hsp70 chaperone protein, called Hsc-70 SBD (18 kDa; τ_c = 14 ns). Few long-range NOEs could be identified unambiguously from the 3D [^{1}H, ^{13}C, ^{1}H] NOESY-HSQC spectrum of this protein, because of extensive assignment degeneracy and broad lines. Consequently, 4D spectroscopy was necessary.

In this paper, we present a theoretical analysis of the performance of the 4D [^{1}H, ^{13}C, ^{13}C, ^{1}H] HMQC-NOESY-HSQC experiment (*1–3*) in terms of effective resolution and sensitivity (Table 1). Effective resolution is defined here as the percentage of all possible NOE cross peaks that can be assigned unambiguously on the basis of spectral data alone. We attempt to answer the following questions: given that the 4D spectrum must be recorded in a fixed amount of time, how should the digital resolution be distributed over the three indirect dimensions? How does that distribution affect effective resolution and sensitivity? How should the spectrum be aliased to acquire such an experiment in reasonable time? What experimental design is best for interpretation? We analyze these issues with computational simulations based on the actual assignment table of Hsc-70 SBD. Although the simulation is performed on a predominantly beta sheet protein, the conclusions concerning the optimal sampling among the indirect dimensions should be the same for all proteins, albeit the maximum percentages of unambiguous assignment will vary. Our analysis gave rise to the design of two 4D NOE experiments that gave the structure-independent assignment of over 914 long-range 4D NOE cross peaks for Hsc-70 SBD (*4*).

DISTRIBUTION OF RESOLUTION—GENERAL CONSIDERATIONS

Our discussion is based on the 4D [^{1}H, ^{13}C, ^{13}C, ^{1}H] HMQC-NOESY-HSQC experiment (*1–3*). We think of the 4D spectrum as a set of 2D ^{13}C–^{1}H origination planes that communicates with a set of 2D ^{13}C–^{1}H destination planes through NOE

[1] To whom correspondence should be addressed. E-mail: zuiderwe@umich.edu.

1090-7807/99 $30.00

TABLE 1
Experimental Parameters

	Acquisition times (750 MHz)			Complex points			Digital resolution (one zero fill)				
Total expt. time	D1	D2	D3	D1	D2	D3	D1	D2	D3	Figure	Comment
27.6 h	13.3 ms	8.3 ms	2.1 ms	72	9	12	0.20 ppm	0.08 ppm	1.25 ppm	3a	Max eff res
29.6 h	10.6 ms	6.7 ms	3.3 ms	58	8	18	0.25 ppm	0.10 ppm	0.80 ppm	3c	High res + sens
8.0 days	13.3 ms	19.6 ms	6.3 ms	72	22	34	0.20 ppm	0.034 ppm	0.42 ppm	4a	Max eff res
8.2 days	13.3 ms	13.9 ms	8.9 ms	72	16	48	0.20 ppm	0.048 ppm	0.3 ppm	4d	High res + sens
8.2 days	8.9 ms	13.9 ms	13.3 ms	48	16	72	0.30 ppm	0.048 ppm	0.2 ppm	4e	Ease of analysis

Note. Parameters pertaining to the optimized triple aliasing scheme with spectral widths of 1.5, 29.0, and 29.0 ppm (D1,D2,D3).

transfer. First we address the distribution of digital resolution over the origination and destination planes. One school of thought suggests that acquired digital resolution is immaterial for the resolution of the experiment; provided that the digital resolution is sufficient to separate the peaks in the vast 4D spectral space, contour interpolation and/or zero filling can provide the precise peak position and thus yield the assignment. However, peak interpolation fails when signal-to-noise ratio is low (*5*), as is common in 4D, and digital resolution becomes a determining factor.

The acquired digital resolution (in this paper assumed to be the spectral width divided by two times the number of complex points acquired assuming a single zero fill) can be used to tabulate the effective resolution of the 2D experiment simply by considering the proton–carbon correlation. The resolution can be represented as a rectangle of the proper dimension centered on each cross peak. If a second peak in the assignment list falls within the rectangle, the assignment cannot be made. It is instructive to plot all potential spectral overlaps on a single plot (Fig. 1). In the center of this figure is the superposition of all the aliphatic resonances from the 18-kDa substrate binding domain (to form a single point), around which all relative positions of the resonances within ± 0.2 ppm in proton chemical shift and ± 2.0 ppm in carbon chemical shift are plotted. The figure is convenient in that a single "resolution rectangle" can be visualized representing an area of ambiguity. With this analysis, only the total area of the 2D resolution rectangle is directly proportional to the number of ambiguities that will occur. The observed uniform distribution of nearest neighbors in carbon and proton dictates that there is no advantage or disadvantage to obtaining spectra with higher resolution in proton or carbon.

This is no longer true considering the full 4D experiment, where the resolution distribution over all dimensions must be considered carefully. Given that the proton digital resolution of the destination plane is high because it is observed directly, the destination plane most likely has a two-dimensional resolution of a shape as indicated in Fig. 2A. It is apparent that the least effective resolution will result when the resolution for the origination plane mimics that of the destination plane, i.e., high proton resolution (Fig. 2A). This is suboptimal because one views 4D data from "both sides": a NOE between, e.g., the pairs C_i–H_i and C_k–H_k is analyzed first with C_i–H_i and C_k–H_k in the origination and destination plane, respectively, followed by analysis of the symmetric cross peak with C_k–H_k in the origination and C_i–H_i in the destination plane, respectively. Thus, if the carbon shift position of, for example, C_k–H_k is unassignable in the destination plane because of low carbon digital resolution, it is still unassignable for the symmetric cross peak in the origination plane if the resolution rectangles are identical in both planes. Therefore, the digital resolution should be designed to be complementary in origination and destination planes, which leads, because of the "gratuitous" directly detected proton high resolution in the destination plane, to an asymmetrically high carbon resolution and low proton resolution in the origination plane. This design is shown in Fig. 2B. The simulations based on real spectral distributions below bear out this conclusion. General limitations in resolution in multidimensional spectra dictate that planes have a certain "thickness," in the case of a 4D spectrum, a two-dimensional thickness, that causes cross talk. For this reason, it is wise to set up the 4D experiment in an asymmetric fashion: it makes that different peaks cause different cross talk in the corresponding origination and destination planes. This allows easier recognition of the cross talk. In practice, it is desirable to have a high resolution in both dimensions of the destination plane as shown in Fig. 2C. This minimizes cross talk in the origination planes when they are displayed for analysis, allowing easy interpretation of the entire 4D data set using a simple graphical interface. This design will also be discussed below.

DISTRIBUTION OF RESOLUTION—SIMULATION

While the above considerations give some intuitive direction to the design of a 4D experiment, it is not clear what the extent of asymmetry should be. Also, the question of how sensitivity is affected by the resolution cannot be answered from the above models. For this reason, the efficiency of the 4D experiments was simulated. A computer program was written that accepted the actual assignment list of Hsc-70 SBD's protons

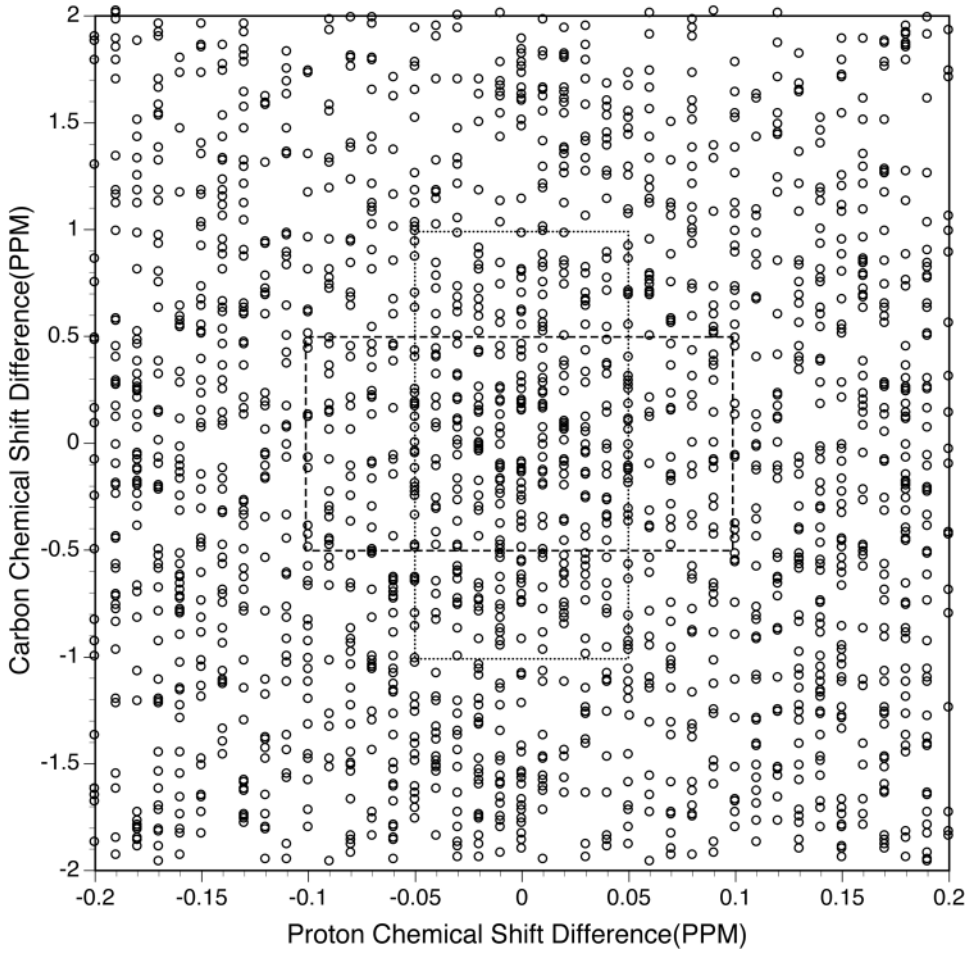

FIG. 1. Ambiguity distribution plot. All cross peaks {i} of the experimental proton–carbon correlation spectrum of Hsc-70 SBD that are within 0.2 ppm in proton shift and 2.0 ppm in carbon shift to every other cross peak {j} are plotted. The cross peaks {j} are superimposed at the origin. Rather than attempting to solve individual cases of overlap in the proton–carbon correlation mapping, this mapping provides a route to a statistical analysis. The two rectangles are "resolution rectangles" representing experiments collected with higher proton resolution (dotted rectangle) and higher carbon resolution (dashed rectangle). All resonances that are "too close" as defined by the digital resolution (inside the rectangle) will be ambiguous. The two rectangles have an equal total number of digitization points and this 2D case always results in a constant area for the rectangle. Both the carbon and the proton chemical shifts were tabulated to the nearest 0.01 ppm resulting in the apparent "stripes" in the proton dimension. This rounding has a negligible effect on the conclusions of the simulation.

and carbons (701 assigned proton (groups) with associated carbons) and which tallied the number of unambiguous assignments out of all possible NOE cross peaks (i.e., 701∗700/2 total, independent of structure) for a given digital resolution. A NOE cross peak was assumed unassignable if a single ambiguity remained for either of the resonances after analyzing the original and symmetric peak.

Figure 3 shows the results for a 4D experiment of limited resolution that may be acquired in roughly 30 h, if optimal aliasing is applied (see below). The figure, which assumes a

FIG. 2. The use of the resolution rectangles for the analysis of the effects of symmetry in the 4D [^{1}H, ^{13}C, ^{13}C, ^{1}H] HMQC-NOESY-HSQC experiment. (A) A highly symmetric experiment with high resolution along both proton dimensions and low resolution along both carbon dimensions. (B) An asymmetric experiment with the high resolution along the destination proton (direct) dimension and along the origination carbon dimension. (C) An asymmetric experiment with high resolution along the destination proton (direct) dimension and the destination carbon dimension. All experiments shown have equal experimental times (total number of complex points). Area 1 represents the intersection of the two regions of resolution and indicates the amount of protons that absolutely cannot be resolved by pure spectroscopic means, considering both of the symmetric peaks in the NOESY. Area 2 represents the amount of protons that may or may not be resolved, depending on the number of overlaps that occur for the other proton involved in the NOE. It is clear that the symmetric experiment in A is not optimal. Experiments B and C are equal in the number of absolute overlaps, but experiment C has a larger total area (from more area 2) and thus more possible secondary overlaps. Although experiment B clearly has the highest effective resolution, experiment C has the advantage of ease of use, as the origination planes can be viewed without cross talk.

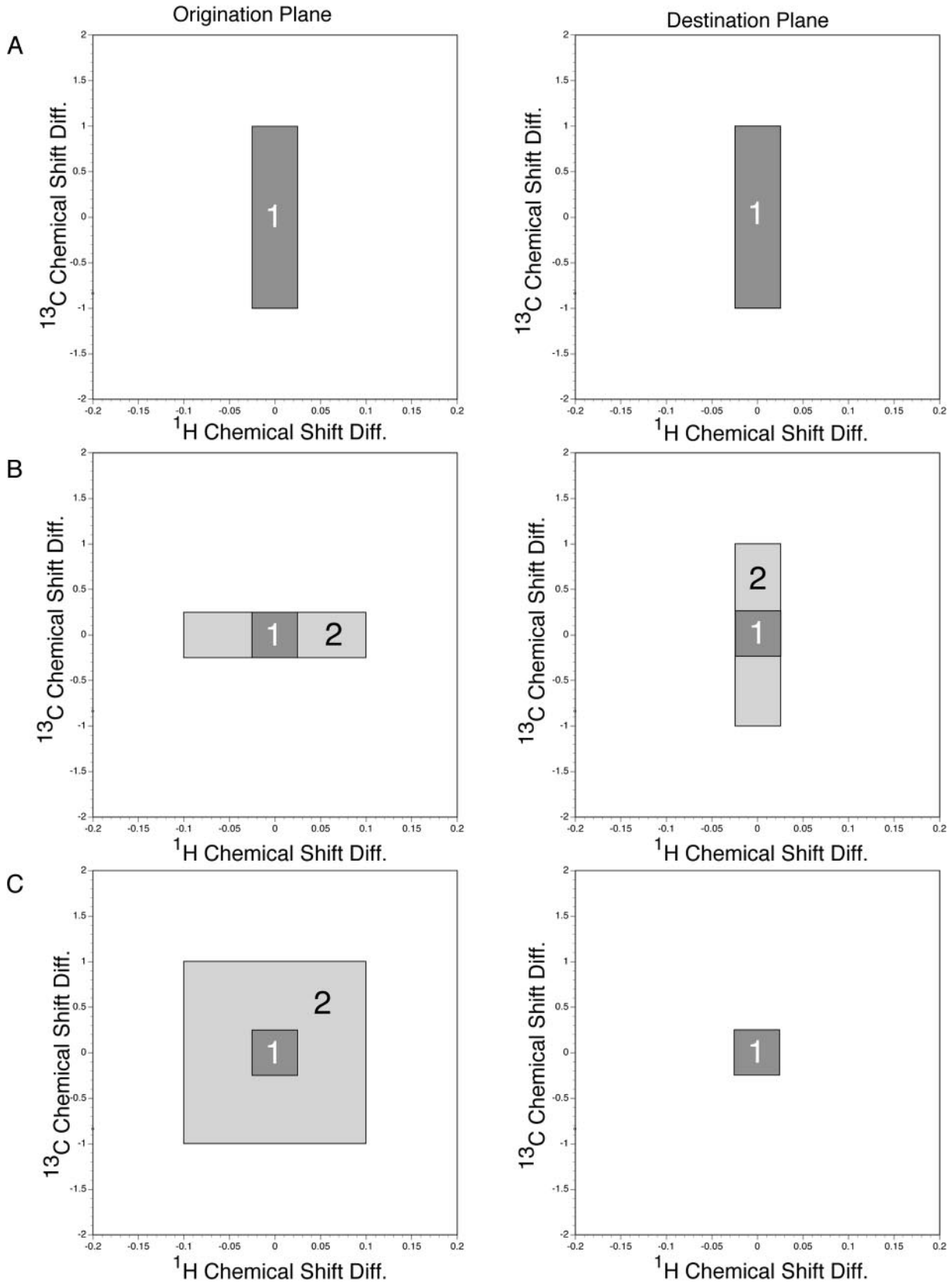
Origination Plane
Destination Plane
A
B
C
1
2
^{13}C Chemical Shift Diff.
^{1}H Chemical Shift Diff.

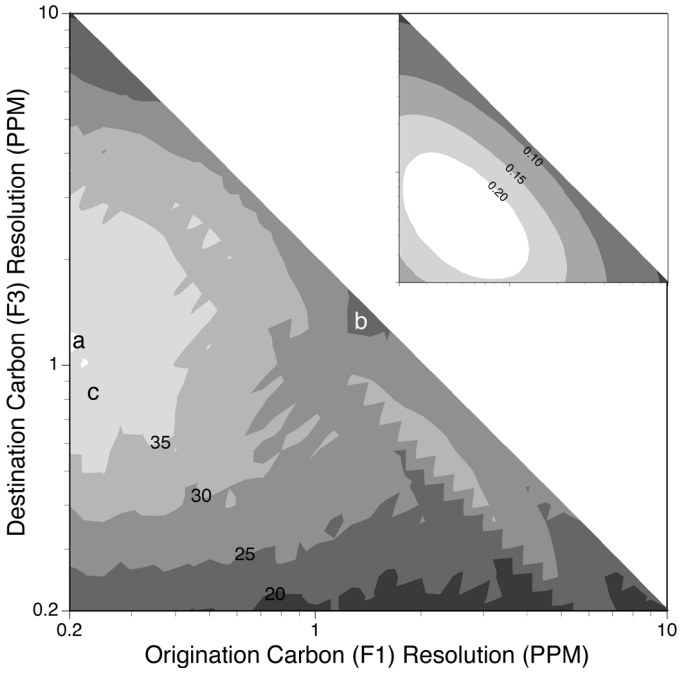

FIG. 3. Computation of resolution and sensitivity as a function of digital resolution in the three indirect dimensions of a 4D [^{1}H, ^{13}C, ^{13}C, ^{1}H] HMQC-NOESY-HSQC experiment. The direct proton resolution was kept at 0.02 ppm/point. A composite resolution of 0.02 ppm^{3}/point^{3} in the three indirect dimensions was maintained while the individual resolutions were varied. The origination proton resolution is thus given by (0.020 / (origination carbon resolution × destination carbon resolution)). The calculation is based on an experimental assignment list of aliphatic protons and carbons of the protein Hsc-70 SBD. The simulation identified all pairs of protons that could be unambiguously assigned at the specified resolutions. Efficiency is indicated as a percentage of unambiguous assignments. This modest 4D experiment, which can be recorded in as little as 30 h using the aliasing scheme shown in Fig. 5, results in a maximum of 40.9% unambiguous identification of all possible pairs of protons, independent of structure. This optimal experimental design is indicated by **a. b** shows a less-than-optimal design maximizing origination proton resolution, resulting in only 24% unambiguous identifications. The insert shows the sensitivity of this 4D experiment compared to nondecaying interferograms as a function of the distribution of resolutions over the same area. **c** indicates an experimental design that is the best compromise between effective resolution and sensitivity.

fixed resolution of 0.01 ppm/point for the destination proton, displays information on all three indirect resolutions as their product is held constant. Thus, improving origination carbon resolution while holding the destination carbon resolution constant, i.e., moving from right to left on the figure, decreases the underlying origination proton resolution. This change is seen to yield a marked improvement in the percentage of assignable resonances, and hence effective resolution, as predicted above. The surprisingly good result, with 41% of all possible NOE cross peaks unambiguously assignable, is obtained for the highest practical origination carbon resolution (0.2 ppm/point) with a 1.0 ppm/point destination carbon resolution and an origination proton resolution of 0.1 ppm/point, as indicated by **a** in the figure. This experimental design is a noticeable improvement over an experiment in which the origination proton resolution is chosen to be high. This design, with a proton resolution of 0.04 ppm/point, generates only 24% unambiguous assignments, as indicated by **b** in the figure. The simulation further shows that the maximum effective resolution in the 4D experiment occurs when the two-dimensional resolution in the origination and destination planes is equal, but oppositely distributed (**a**).

Using the same program, we compute for a three-dimensional [^{1}H, ^{13}C, ^{1}H] NOESY-HSQC spectrum (assuming a 750-MHz instrument with acquisition times of 66, 13.3, and 66 ms for ^{1}H(F_1), ^{13}C(F_2), and ^{1}H(F_3), respectively) of this protein that a maximum of only 9% of all possible NOE cross peaks can be assigned unambiguously from spectral data alone. This *did* include analysis of the symmetrically related (transposed) peak, but, like the 4D simulations, *did not* include interpolation beyond the digital resolution and linewidth.

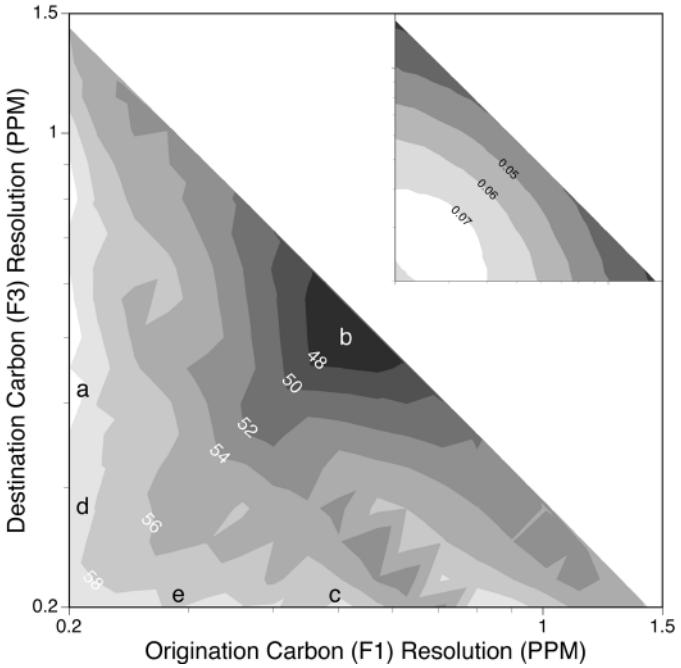

FIG. 4. Computation of resolution and sensitivity as a function of digital resolution in the three indirect dimensions of a 4D [^{1}H, ^{13}C, ^{13}C, ^{1}H] HMQC-NOESY-HSQC experiment. Conditions were as for Fig. 3, but a composite resolution of 0.00285 ppm^{3}/point^{3} in the three indirect dimensions was maintained. The origination proton resolution is thus given by (0.00285/ (origination carbon resolution × destination carbon resolution)). Efficiency is indicated as a percentage of unambiguous assignments. This optimized 4D experiment, which can be recorded in 8.2 days using the aliasing scheme shown in Fig. 5, results in a maximum of 61% unambiguous identification of all possible pairs of protons, as indicated by **a. c** identifies an alternative design maximizing destination carbon resolution, resulting in 58% unambiguous identifications, but with easier interpretation using a graphical interface (see text). The conditions indicated by **b,** with high proton resolution, are suboptimal. The inset shows the sensitivity of this 4D experiment compared to nondecaying interferograms as a function of the distribution of resolutions over the same area. **d** and **e** give the best compromise of effective resolution and sensitivity.

A major concern is whether the high effective resolution in 4D spectroscopy has the traditional association with low sensitivity. The sensitivity of the different experimental designs was computed from the product of the areas of the three decaying interferograms relative to the product of nondecaying interferograms. Linewidths of 50 Hz for carbon and 30 Hz for proton were assumed in order to compute the decays, which are representative for larger proteins with a correlation time of 15 ns, including the effects of unresolved scalar couplings (*6*). The results of these computations are shown as an insert in Fig. 3. It is very encouraging to observe that the area of high sensitivity roughly overlaps with the area of maximum effective resolution (**c**).

Whether this 30-h 4D experiment has sufficient practical sensitivity is of course determined by protein concentration, correlation time, and (ever increasing) spectrometer sensitivity. The counterintuitive effect of simultaneous occurrence of maximum sensitivity and resolution is the result of the high intrinsic resolution of the 4D experiment even at low digital resolution of the individual interferograms. In contrast, higher effective resolution in lower dimensionality experiments can only be achieved when the indirect interferograms are collected to long acquisition times, yielding low sensitivity. Four-dimensional spectra emphasizing high proton resolution have appeared in the early literature of 4D experiments (*1–3*). This results in less-than-optimal effective resolution and sensitivity in this design as disclosed by Fig. 3.

Figure 4 shows the effective resolution of a high-resolution 4D experiment, which may be acquired in roughly 8 days, if optimal aliasing is applied (see below). The highest achievable resolution, with in excess of 60% of all possible NOE cross peaks assignable unambiguously, is obtained for parameters indicated by **a** in this figure. Again, it is evident from the figure that the effective resolution of the experiment decreases with an increase in origination proton resolution, i.e., moving from the bottom left toward **b.** Relative sensitivity in the experiment is given in the insert. Combining the resolution and sensitivity information in Fig. 4, one concludes that the best experimental design is given by the parameters indicated with **d.** The overall sensitivity of this high-resolution 8-day experiment will be approximately equal to that of the 30-h experiment. For the 8-day experiment it is largely irrelevant in which carbon dimension the digital resolution is placed (as long as it is not in the indirect proton dimension). Therefore, it is possible to set up the experiment with good destination carbon resolution, as indicated by **c** (best resolution) and **e** (best sensitivity compromise). This is an important property that allows for straightforward analysis using standard NMR display software. With high destination resolution, the two destination frequencies for a NOE in the 4D spectrum can be selected with precision, allowing the display of the corresponding origination frequencies in a 2D plane that is free of cross talk.

MINIMIZATION OF THE FREQUENCY SPACE

Up to this point, the discussion was focused on obtaining a maximum resolution with a fixed amount of experimental time and spectral widths. This section will describe an intricate aliasing design aiming to minimize the frequency space that must be sampled, thus maximizing the digital resolution obtainable in a given experimental time. The discussion is again based on the 4D [^{1}H, ^{13}C, ^{13}C, ^{1}H] HMQC-NOESY-HSQC experiment that can be recorded with two scans per increment as described by Vuister *et al.* (*3*). A proposal for aliasing in the origination plane is shown in Fig. 5. Based on the proton–carbon correlation of Hsc-70 SBD shown in Fig. 5A, it is clear that the effective proton spectral width for a given carbon chemical shift is usually less than 1.5 ppm. Aliasing the proton spectral width of 8 ppm with a window of 1.5 ppm introduces only an additional 1.5% ambiguities compared to the unaliased spectrum. The result of this procedure is shown in Fig. 5B. At this point, it may appear as if no additional aliasing should be executed. However, an aliasing of the 140-ppm carbon spectrum with a 29-ppm window (4.83-fold) as indicated in the figure can be easily accommodated if the sign of the folded peaks is distinguished by a negative intensity afforded by a 180° first-order phase correction (*7*). Of course, mutual cancellation of peaks in the 2D plane in Fig. 5C appears excessive and forbidding; however, in a full 4D spectrum only a small number of resonances will appear in each origination plane and chances of cancellation are remote. If such an overlap would nevertheless occur, it may result in the loss of two cross peaks rather than introducing a new ambiguity, a small price to pay for better resolution for the majority of the peaks.

An identical phase-alternated aliasing for the carbons in the destination plane, with (obviously) no aliasing along the directly detected destination protons, is presented. In this design, all diagonal peaks have the same phase, which has a practical advantage with respect to phasing and baseline correction. The final spectral widths for this optimized triple aliasing are 1.5, 29.0, and 29.0 ppm about carrier positions of 4.85, 30.5, and 30.5 ppm for origination proton, origination carbon, and destination carbon, respectively. This optimal design thus represents a 124-fold reduction in spectral space, to be compared with the aliasing designs by Clore *et al.* (*1*) (46-fold), Zuiderweg *et al.* (*2*) (15-fold), and Vuister *et al.* (*3*) (46-fold). With our procedure, as outlined in the legend to Fig. 5, the experiment of Fig. 3 can be collected in about 28 h and the experiment of Fig. 4 in 8.2 days.

DEMONSTRATION OF TRIPLE ALIASING

To demonstrate the effectiveness of the discussed resolution distribution and the triple aliasing scheme, a 4D [^{1}H, ^{13}C, ^{13}C, ^{1}H] HMQC-NOESY-HSQC experiment was collected for a 1.5-mM sample of double-labeled 18-kDa Hsc-70 SBD in $^{2}H_2O$. At the measuring temperature of 25°C the protein has a

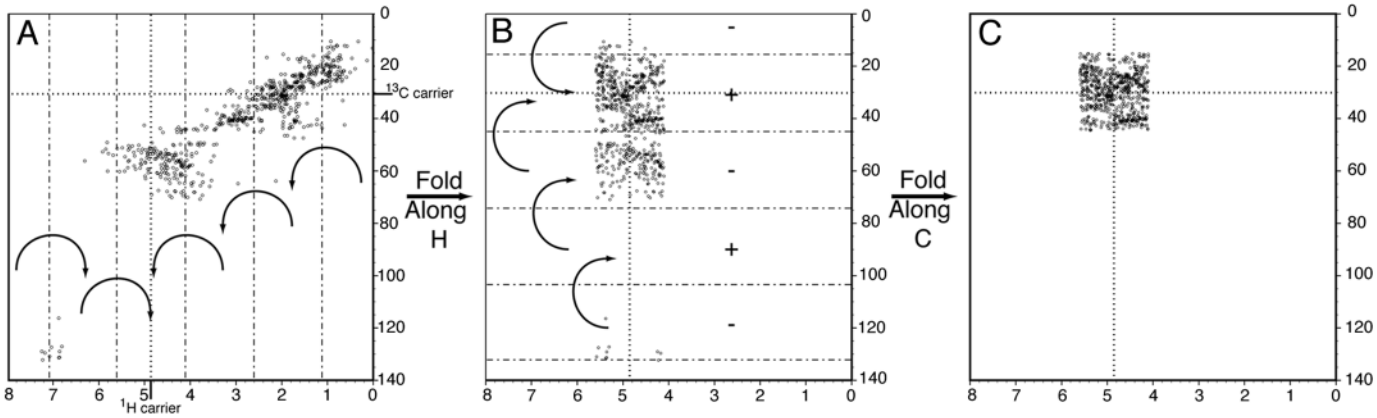

FIG. 5. Simulations of aliasing in the origination plane using the 2D peak positions from the proton–carbon correlation spectrum of the 18-kDa protein Hsc-70 SBD. A, the full correlation spectrum; B, 5.33-fold aliasing in the ^{1}H dimension, not using phase encoding, resulting in an additional 1.5% of peak overlap; C, additional 4.83-fold aliasing in the ^{13}C dimension, using first-order phase encoding. Note that the aliasing in carbon introduces few if any ambiguities, while the aromatics are placed well in the spectrum (observe the sign of the regions of superposition). The carrier positions are indicated by the cross of dotted lines. The carbon carrier is optimized for detecting methyl NOEs. The resulting distribution of data in C is nearly uniform, resulting in a highly efficient use of the sampling in frequency space. The aliasing scheme thus results in a 26-fold reduction of origination plane sampling space. When combined with identical aliasing in the destination carbon dimension, a total of a 124-fold reduction in the combined indirect dimensions is achieved. This aliasing allows the spectrum of Fig. 3 to be collected in approximately 28 h as is computed as follows. The full carbon and proton spectral widths are 140 and 8 ppm, respectively. The desired origination carbon resolution is 0.2 ppm/point, the origination proton resolution is 0.1 ppm/point, and the destination carbon resolution is 1.0 ppm/point. In order to acquire this resolution, not allowing for any zero-filling in processing, one needs 140/0.2∗8/0.1∗140/1 = 7,840,000 (not complex) increments. Using the proposed triple-aliasing scheme that reduces indirect spectral space 124-fold, only 63,226 noncomplex increments are needed (which translates to 7903 hypercomplex increments). With the minimal phase-cycle of two scans (*3*) and an average duration of 0.8 s per increment, one thus computes 63,226∗2∗0.8 / 3,600 = 28 h for the experiment. The experiment of Fig. 4 has seven times better resolution and will hence take seven times as long (8.2 days).

fairly long correlation time of 14 ns. The experiment was recorded in 5.5 days on a Bruker DMX 750-MHz instrument using spectral widths of 2.85, 31.86, and 31.86 ppm for the origination proton, origination carbon, and destination carbon dimension, respectively. The 2.85-ppm spectral width in proton (rather than 1.5 ppm) was used to maintain a high sensitivity. A digital resolution (assuming a single zero fill in each indirect dimension) of 0.09, 0.45, and 0.24 ppm/point was obtained for origination proton, origination carbon, and destination carbon, respectively. The destination carbon was collected at high resolution (rather than origination carbon) to allow easy interpretation using a graphical interface as explained above. An origination plane displaying all NOEs to VAL 104γ' is shown in Fig. 6. The degeneracy of the peak assignment is given in parentheses. It is clear that the low intrinsic digital resolution and superposition of peaks due to the multiple aliasing in this plane is not a problem.

The experiment was collected with high resolution in the carbon destination dimension resulting in 39% unambiguous identifications. Together with a 4D [^{1}H, ^{13}C, ^{15}N, ^{1}H] HMQC-NOESY-HSQC experiment (*8*) with the same aliasing in the origination plane, the 4D spectra yielded 1867 unambiguously defined NOEs (914 long range) on which the structure calculation of Hsc-70 SBD was based (*4*). Subsequent extensive analysis of several 3D NOE spectra yielded only 672 additional long-range NOEs for a refined structure based on a total of 4150 NOEs.

CONCLUSIONS

In this paper, we have demonstrated, by simulation and experiment, that asymmetric 4D [^{1}H, ^{13}C, ^{13}C, ^{1}H] HMQC-NOESY-HSQC spectra result in a substantially higher number of completely unambiguous NOE assignments than the commonly used symmetric experiments. In addition, a unique asymmetric aliasing pattern is presented. These methods, when combined, will significantly decrease the experimental time and improve the effective resolution of the 4D [^{1}H, ^{13}C, ^{13}C, ^{1}H] HMQC-NOESY-HSQC. The asymmetric version of a typical 4D experiment with digital resolutions of 0.09, 0.2, and 1.1 ppm/point for the origination proton, origination carbon, and destination carbon, respectively, results in 41% completely unambiguous assignments for all possible NOEs. This is the experiment of choice when limited instrument time is available: the experiment can be recorded in a little more than a day with the proposed aliasing scheme. The experiment can be repeated with more scans for higher sensitivity if more instrument time is available. If intrinsic sensitivity allows, more instrument time can also be utilized to acquire an experiment with higher effective resolution. For that case placing high resolution in the destination carbon is recommended. The main benefit of this experiment is that it can be analyzed in a straightforward manner using a simple graphical interface. Such a 4D experiment is achieved in 8 days, using the aliasing scheme suggested, with resolutions of 0.02, 0.8, and 0.2 ppm/

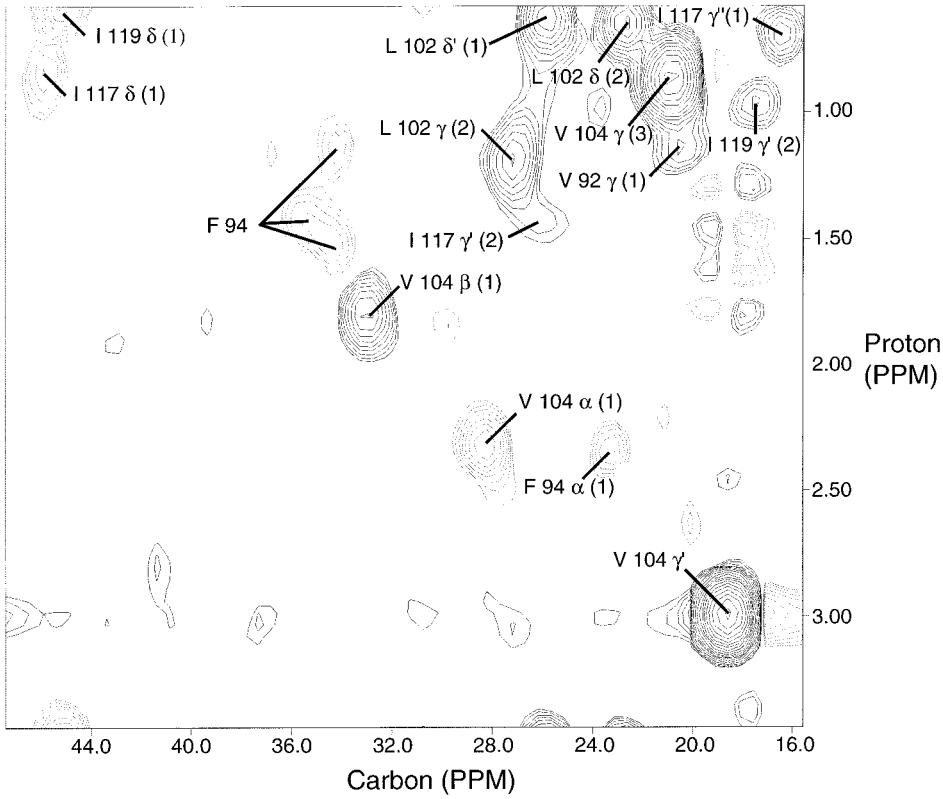

FIG. 6. Originating plane for the destination resonance of Valine 104γ′ of Hsc-70 SBD obtained from the high-resolution 4D [^{1}H, ^{13}C, ^{13}C, ^{1}H] HMQC-NOESY-HSQC spectrum (mix: 75 ms), recorded in 5.5 days on a Bruker DMX750 spectrometer. The pulse sequence as described by Vuister *et al.* (*3*) was used, with two scans per increment. The plane is taken at the frequencies 18.92 (F_3) and 0.13 (F_4). The large peak at (18.92, 3.0) ppm is the (aliased) diagonal. The following acquisition parameters were used for τ_1(^{13}C), τ_2(^{1}H),τ_3(^{13}C), and τ_4(^{1}H) respectively: spectral widths, 31.86, 2.85, 31.86, and 16.0 ppm; complex points 34, 16, 64, and 512; acquisition times 5.69, 7.49, 10.71, and 42.67 ms; carriers 31.50, 4.86, 31.50, and 4.86 ppm. A recycling delay of 0.7 s was used. The F_2(^{1}H) spectral width was relatively large, and consequently the τ_2 time was short, to enhance the overall sensitivity of the experiment.

point for the origination proton, origination carbon, and destination carbon, respectively. This experiment generates 60% unambiguous assignments.

ACKNOWLEDGMENTS

This work was supported by NIH Grant RO1-GM052421. The experimental 4D data were acquired at the National NMR Facility at Madison, Wisconsin. We acknowledge Dr. Frits Abildgaard for expert assistance. We thank Dr. Gregory Flynn for the sample of Hsc-70 SBD.

REFERENCES

1. G. M. Clore, L. E. Kay, A. Bax, and A. M. Gronenborn, *Biochemistry* **30,** 12–18 (1991).
2. E. R. P. Zuiderweg, A. M. Petros, S. W. Fesik, and E. T. Olejniczak, *J. Am. Chem. Soc.* **113,** 370–372 (1991).
3. G. W. Vuister, G. M. Clore, A. M. Gronenborn, R. Powers, D. S. Garrett, R. Tschudin, and A. Bax, *J. Magn. Reson. B* **101,** 210–213 (1993).
4. R. C. Morshauser, W. Hu, H. Wang, Y. Pang, G. Flynn, and E.R.P. Zuiderweg, *J. Mol. Biol.* **289,** 1387–1403.
5. J. C. Hoch and A. S. Stern, “NMR Data Processing,” p. 174, Wiley–Liss, New York (1996).
6. G. Wagner, *J. Biomol. NMR* **3,** 375–385 (1993).
7. M. Ikura, L. E. Kay, R. Tschudin, and A. Bax, *J. Magn. Reson.* **86,** 204–208 (1990).
8. L. E. Kay, G. M. Clore, A. Bax, and A. M. Gronenborn, *Science* **249,** 411–414 (1990).